Fully Automatic Deformable Model Integrating Edge, Texture and Shape
Application to Cardiac Images Segmentation

Clément Beitone[1,3], Christophe Tilmant[1,3] and Frédéric Chausse[2,3]

[1]*Clermont Université, Univ. Blaise Pascal, Institut Pascal, BP 10448, F-63000 Clermont-Fd, France*

[2]*Clermont Université, Univ. d'Auvergne, Institut Pascal, BP 10448, F-63000 Clermont-Fd, France*

[3]*CNRS, UMR 6602, Institut Pascal, F-63171 Aubière, France*

Keywords: Fully Automatic Segmentation, Deformable Model, MRI, Weibull Model, Monogenic Signal.

Abstract: This article presents a fully automatic left ventricle (LV) segmentation method on MR images by means of an implicit deformable model (Level Set) in a variational context. For these parametrizations, the degrees of freedom are: initialization and functional energy. The first is often delegated to the practician. To avoid this human intervention, we present an automatic initialisation method based on the Hough transform exploiting spatio-temporal information. Generally, energetic functionals integrate edges, regions and shape terms. We propose to bundle an edge-based energy computed by feature asymmetry on the monogenic signal, a region-based energy capitalizing on image statistics (Weibull model) and a shape-based energy constrained by the myocardium thickness. The presence of multiple tissues implies data non-stationarity. To best estimate distribution parameters over the regions and regarding anatomy, we propose a deformable model maximizing locally and globally the log-likelihood. Finally, we evaluate our method on MICCAI 09 Challenge data.

1 INTRODUCTION - STATE OF THE ART

Cardiovascular diseases are the main cause of death on earth. According to the World Health Organization in 2008, they are responsible for 30% of the total number of deaths. Systolic function impairment and especially the left ventricle (LV) is one of the main characteristics reflecting that the heart is damaged. Quantitative analysis provides important cardiac functional parameters for heart disease diagnosis, for example the *strain* showed is reliable prognostic value.

The evaluation of these parameters requires, among other things, to have an accurate segmentation result. This step has been the subject of a large number of studies: a review and an evaluation of segmentation methods applied to MR images can be found in (Petitjean and Dacher, 2011).

Authors propose the following segmentation methods classification regarding the level of external information they require (strong/weak) and their methodological approach:

Weak Priors	Strong Priors
(i) Image-based	(a) AAM
(ii) Pixel classification	(b) Atlas-based
(iii) Deformable models	(c) Shape Prior

We propose a variational method, belonging to the deformable model category with weak priors (iii), in order to segment LV. There are three degrees of freedom: parametrization, initialization and energy functional.

We decided to represent our deformable model using the level set framework because it allows topological changes. These issues arise, for example, when there are papillary muscles inside the endocardium cavity.

Deformable model evolution is linked to an optimisation problem. The functional minimization is
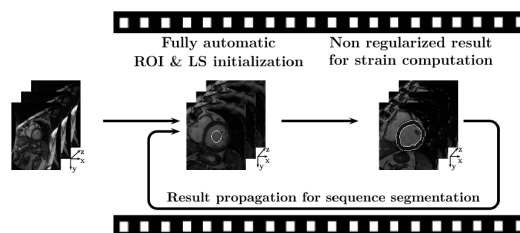

Figure 1: Overall scheme of the proposed method.

achieved using a descent method, and leads to a local minimum dependent on the initialization. Usually, this step is delegated to the practician (Lu et al., 2009). Nevertheless, this tedious intervention can be automated using the geometrical properties of the left cavity (quasi-conic shape); which can be approximated by a circular shape in a basal short axis (SAX) slice. Heart motion is also discriminant to initialize the model (Pednekar et al., 2006).

Using a deformable model requires to design an energy functional which depends on internal information (regularization) and external information (image, prior). For example, the geodesic model (Caselles et al., 1997) uses a functional dependent on the image gradient intensity. The key idea behind *edge-based energy* is to force the model to converge on areas where the gradient intensity is high, i.e where edges are. The authors also proposed to work on image texture by integrating *region-based energy*. The seminal Chan and Vese method (Chan and Vese, 2001) minimizes inter-class variance on pixels inside/outside the model. Some generalizations exploit statistics linked to the physical process of the image formation. For example, the Weibull model (Ayed et al., 2006) allows to model different distributions which can be used to finely characterise regions. To solve the non-stationarity issue induced by region response, Lankton *et al.* (Lankton and Tannenbaum, 2008) propose a local region energy. In this method, statistics are evaluated along the deformable model. However in real images, noise and missing data require to incorporate geometrical constraints in the method, known as *shape-based energy*, to solve these issues. This prior information can be integrated in different ways into the variational method. For example, Foulounneau (Foulonneau et al., 2003) uses a mean square process over Legendre moments between the current model shape and a reference shape. One of the main interests of the variational context is its ability to glue different constraints (edge, region and shape-based). This coupling allows to strengthen the method by merging information sources. For example the Geodesic Active Region (GAR) model proposed by Paragios (Paragios and Deriche, 2002) is one of the first to propose an edge/region-based energy.

A large number of methods apply these energies to segment cardiac images. Ultrasound scans (US) uncovered specific needs for these noisy and poorly contrasted images. Some authors developed frameworks to replace gradient-based methods. For instance, some methods use the monogenic signal and the asymmetry measure (Felsberg and Sommer, 2001; Kovesi, 1997) to segment cardiac ultrasound images with an edge-based energy (Rajpoot et al., 2008). In

a region-based context Barbosa *et al.* (Barbosa et al., 2013) used Lankton approach with Rayleigh statistics in order to segment US images. The prior knowledge of the heart geometry can be used in a shape-based energy. This kind of anatomical constraint was proposed by Paragios (Paragios, 2002) in MRI left ventricle segmentation by imposing a minimal thickness of the myocardium wall. Finally, Belaid (Belaid et al., 2011) proposes to merge edge (monogenic signal) and region-based (Rayleigh distribution) energy to perform US left ventricle segmentation.

In section 2, we present a general framework to segment LV in MRI (3D+T)(the framework overall is presented on figure 1). In this framework a fully automatic initialization step is performed. Our intention is to apply the ultrasound approach to MRI by carving data terms coherent with the underlying image physics. For that, our functional couples region-based (Weibull model), edge-based (Kovesi asymmetry measure) and shape-based (myocardium wall thickness) energy terms. Its particularity is that we do not use strong prior (spatio-temporal) as in atlas methods. In section 3, we present some results and we compare our method with one of the best methods of the MICCAI 09 challenge.

2 FULLY AUTOMATIC SEGMENTATION

2.1 Deformable Model Framework

The variational formulation of the segmentation problem by means of a deformable model is stated as:

$$\mathcal{S} = \underset{\mathcal{S}^* \in \mathcal{F}_{\mathcal{S}}}{\arg\min} E(\mathcal{S}^*) \Leftrightarrow \frac{\delta E(\mathcal{S})}{\delta \mathcal{S}} = 0 \qquad (1)$$

In our case $\mathcal{S}$ corresponds to the final shape of our model. This shape is taken from a family of solutions $\mathcal{F}_{\mathcal{S}}$, by minimizing the energetic functional E. This optimization problem is solved by means of descent method on an artificial temporal parameter t. The model is put into motion, it is a deformable model:

$$\frac{\partial \mathcal{S}}{\partial t} = -\frac{\delta E}{\delta \mathcal{S}} = V\mathbf{n} \qquad (2)$$

This problem is equivalent to a front propagation where the variation is homogeneous to a speed V on the normal $\mathbf{n}$. The calculus of variations on E can be computed using shape derivative tools (Aubert et al., 2003). In the level set framework, Sethian (Sethian, 1999) showed that this problem can be stated as:

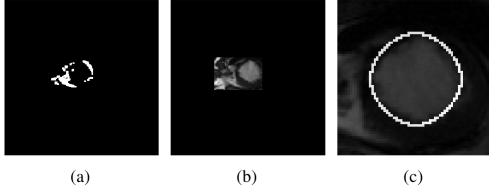$$\frac{\partial \phi}{\partial t} = V|\nabla \phi|, \qquad (3)$$

Figure 2: (a) Motion between ED and ES (b) Motion bounding box (c) Model Initialisation.

where ϕ, the level representation, is a higher order function and $\phi^{-1}(0) = \mathcal{S}$.

2.2 Automatic Initialisation

To initialize our deformable model, we exploit both geometric and motion information. These data are more meaningful when you examine the heart: (i) on a basal SAX slice (ii) between the end of diastole (ED) and the end of systole (ES).

To detect the LV we use a circular Hough transform on ED basal slice but we restrict voting points to a region of interest encompassing strong motion between ED and ES. We select a basal slice in order to be close to our circular shape hypothesis for the LV. The diameter associated to the circular detection is based on myocardium mean size on a basal SAX slice, which is about 50 mm for a healthy adult heart. For that, we restrict the detection to a range of 40 to 60 mm. Our deformable model is initialized using the fast marching method (Sethian, 1999), on a circle with a diameter equal to 95% of the detected diameter. The whole segmentation is carried out on a 80 x 80 mm region of interest centered on the detection. This process is illustrated on Figure 2.

For other slices we propagate the basal result, on which we apply a scale factor following a conical hypothesis (based on the LV shape). Finally, we propagate the segmentation result at time t to initialize the $t+1$ model.

2.3 Functional Definition: Energy Coupling

To segment endocardium and epicardium contours, we use two deformable models based on the coupling three kinds of energy region, edge and shape energies:

$$\begin{cases} E_{endo} & = \alpha_1 E_{R_{endo}} + \alpha_2 E_E \\ E_{epi} & = \beta_1 E_{R_{epi}} + \beta_2 E_E + \beta_3 E_A \end{cases} \quad (4)$$

E_{endo} and E_{epi} correspond respectively to energies used to segment endocardium and epicardium contours. $E_{R_{endo}}$ and $E_{R_{epi}}$ correspond to region-based terms, E_E is an edge-based term and E_A is a shape

term. Parameters α_i and β_i are used to weigh the influence of each term.

Edge-based energy: Our edge-based energy data term is the same for both segmentations. This data term is based on a geodesic model, however, we use a step edge detector based on phase information instead of a classic gradient-based detector:

$$E_E = \int_S g\left(FA(I_{NL})\right) d\mathbf{x} \quad (5)$$

where $\mathbf{x}$ is a given point, $g(a) = \frac{1}{1+a^2}$ and I_{NL} is the locally normalized input image. The edge detector FA, is the feature asymmetry introduced by Kovesi (Kovesi, 1997). This measure gives reliable, well localized but incomplete edges even in noisy images. We also used the monogenic signal (Felsberg and Sommer, 2001), the multidimensional extension of the 1D analytic signal, to replace steerable filters used by Kovesi as in (Belaid et al., 2011).

We apply a local normalization filter on the MRI raw image in order to uniformize the mean and variance of an image around local neighbourhoods. This is especially useful for correcting non-uniform illumination or shading artifacts.

Region-based Energy. Our region energy terms are based on a Weibull model (Ayed et al., 2006). The probability density function of a Weibull random variable is:

$$P_W(u) = \frac{\beta}{\eta} \left(\frac{u}{\eta}\right)^{\beta-1} e^{-\left(\frac{u}{\eta}\right)^{\beta}} \times \mathbb{1}_{[0,+\infty[}(u), \quad (6)$$

where η is a scale parameter and β is a shape parameter. This model tends to maximize the log-likelihood of a Weibull distribution over a region $\mathbf{R}$:

$$E_{GW}(\mathbf{R}) = \int_{\mathbf{R}} \log(P_W(I|\mathbf{R})) d\mathbf{x} \quad (7)$$

A local version (Lankton framework) of this global energy might be stated, using a ball $\mathcal{B}$, as:

$$E_{LW}(\mathbf{R}_S) = \int_S \int_{\mathbf{R}_S} \mathcal{B}(\mathbf{x};\mathbf{y}) \log(P_W(I|\mathbf{R}_S)) d\mathbf{y} d\mathbf{x} \quad (8)$$

Global methods provide more energy but are meaningful if the distribution over the considered object follows a stationary process. Nevertheless, our images present some non-stationarity over the myocardium and over its neighbourhood. Experimentally, we show that the distributions over the different regions (using expert segmentations) might be represented as in Figure 3. This figure, shows that myocardium and tissues distributions can be approximated using a normal law and an exponential law.

Cavity distribution can be approximated using a normal law under the assumption that papillary muscles are excluded from the cavity. Indeed, in Figure 3 the intensity step between 20 and 60 comes from the inclusion of these muscles by the expert. We build our region-based energy terms using these observations and assumptions. The final model we used is stated as:

$$E_{R_{endo}} = E_{GW}(\mathbf{R}_S) + E_{LW}(\overline{\mathbf{R}}_S) \tag{9}$$

$$E_{R_{epi}} = E_{LW}(\mathbf{R}_S) + E_{LW}(\overline{\mathbf{R}}_S) \tag{10}$$

In these models, we capitalize on the relative stationarity over the cavity to lead the contour during the first segmentation step and then we work more finely over the remaining tissues (myocardium and its environment). The Weibull scale parameters for the different regions $\mathbf{R}$ are computed (depending if they are global G or local L) as:

$$\eta_{G\mathbf{R}} = \left(\frac{\int_{\mathbf{R}} I^{\beta_{\mathbf{R}}} d\mathbf{x}}{\int_{\mathbf{R}} d\mathbf{x}} \right)^{\frac{1}{\beta_{\mathbf{R}}}}$$

$$\eta_{L\mathbf{R}}(\mathbf{x}) = \left(\frac{\int_{\mathbf{R}} \mathcal{B}(\mathbf{x};\mathbf{y}) I^{\beta_{\mathbf{R}}} d\mathbf{y}}{\int_{\mathbf{R}} \mathcal{B}(\mathbf{x};\mathbf{y}) d\mathbf{y}} \right)^{\frac{1}{\beta_{\mathbf{R}}}} \tag{11}$$
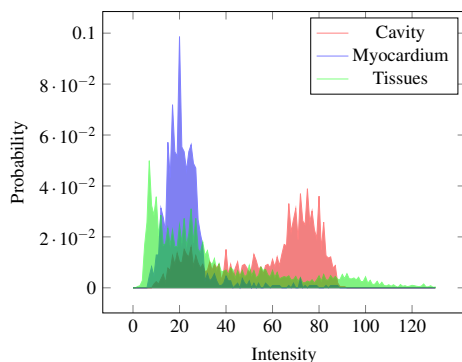

Figure 3: Regions histograms based on an expert segmentation.

Shape-based Energy. Our anatomical constraint is similar to the one introduced by Paragios (Paragios, 2002). This constraint corresponds to a coupling force added back to the global energy to ensure the endocardium segmentation when region and edge-based terms failed. This happens, for example, where the contrast is poor between organs surrounding the heart and the myocardium wall. This force allows to have a non-zero wall thickness for the LV.

This term can be considered as a balloon force with an intensity C depending on the location $\mathbf{x}$ and the endocardium contour position ϕ_{endo}:

$$E_A = \int_{\mathbf{R}_S} C_A(\mathbf{x}, \phi_{endo}) d\mathbf{x} \tag{12}$$

We define C_A, the coupling function as $C_A(\mathbf{x}, \phi_{endo}) = -1$ if $d(\mathbf{x}, \phi_{endo}) < m$, 1 if $d(\mathbf{x}, \phi_{endo}) > M$ and 0 elsewhere. This repulsive force halts the contour propagation if into does not fall in an acceptable distance range. This range $[m, M]$ is defined using standard anatomical wall thickness properties and is determined relatively to the endocardium position.

3 RESULTS & PERSPECTIVES

We assessed our method on the MICCAI 2009 challenge database, which contains 15 patients for the training set and 15 for the validation set. For each patient 6 to 12 SAX slices from the atrioventricular ring to the apex (thickness= 8 mm, gap=8 mm) are given. The spatial resolution is 1.25 mm. For each patient endocardial and epicardial contours were segmented by an experienced cardiologist in all slices at ED and ES phases. Our algorithm was implemented using the ITK Library. Outcome results were obtained using the same parameter set for all patients. The process, for each patient, takes less than a minute to complete.

Comparing our method to the state of the art was a challenging task as the MICCAI ground truth is done by experts who have done smooth manual segmentations. Nevertheless, we here provide segmentation results visually validated by our experts. Secondly, we use the Dice similarity coefficient (DSC) to compare our method with one of the best fully automatic methods of the challenge proposed by (Jolly et al., 2009) and belonging to the category (i). As the DSC measure the amount of overlap between the segmentation and the ground truth, this evaluation is not in favour of our non regularized method. Hence, these results are only here to show that we provide equivalent results.

Visual Assessment. Figure 4 shows segmentation results for patient SC-HF-NI-07 at ED. As can be seen, contours are weakly regularized as expected and the method also works for apical slices.

Figures 5 and 6 present some results from a full sequence segmentation for patient SC-HF-I-05. We can see that the method is quite reliable and provides good LV contours at all time points even for apical slices.

Quantitative Assessment. Table 1 sums up some results for each kind of patient (Heart Failure (HF) Ischemic/Non-Ischemic, Hypokinesis and Normal) and for Training and Validation set. As can be seen,
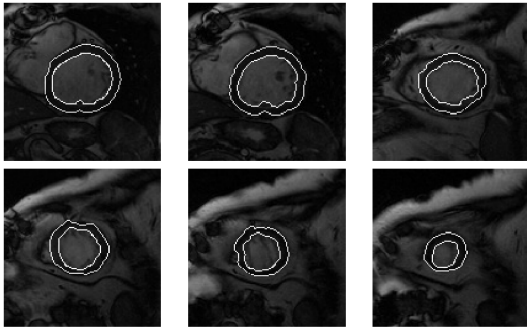
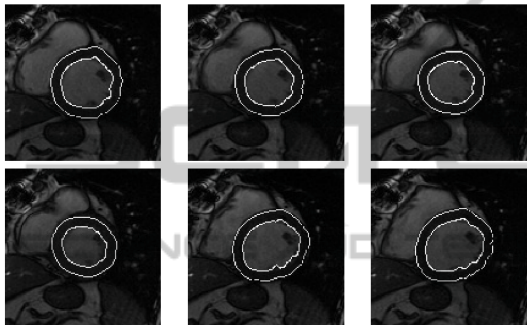Figure 4: ED for patient SC-HF-NI-07 (basal to apical slices).

Figure 5: Full cardiac cycle segmentation from ED to ES and from ES to ED for patient SC-HF-I-05 basal slices.
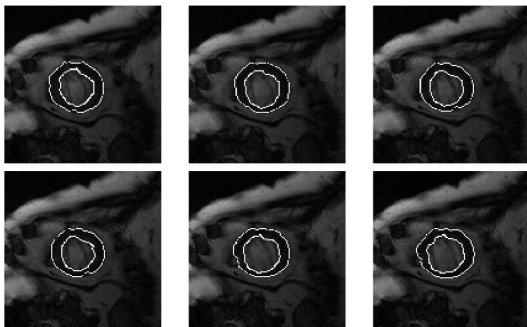

Figure 6: Full cardiac cycle segmentation from ED to ES and from ES to ED for patient SC-HF-I-05 apical slices.

our method gave comparable results to this method. On 30 patients our automatic initialization fails only for patient SC-N-40 which leads to a bad segmentation result.

As we expected, our results differ slightly from those of Jolly. These differences flow from our need of non regularized segmentation results and from the use of the DSC to compare the methods. Nevertheless, our results are coherent with our clinical context, in which papillary muscles must be included inside the myocardium for dense strain computation.

Multi-modal Perspective. Finally, to demonstrate

Table 1: Dice on Training and Validation set.

Patient	Jolly		Proposed method	
	Endo	Epi	Endo	Epi
SC-HF-I-02	0.89	0.94	0.9	0.91
SC-HF-NI-04	0.91	0.95	0.88	0.9
SC-HYP-03	0.90	0.94	0.85	0.89
SC-HF-I-08	0.87	0.93	0.87	0.88
SC-HF-NI-11	0.91	0.94	0.9	0.92
SC-HYP-08	0.86	0.91	0.88	0.88
SC-N-06	0.87	0.95	0.87	0.86

the versatility of our energy and its multi-modal perspective, Figure 7 presents successful segmentation of endocardium and epicardium regions on a two-cavity US slice by simply adapting the β parameters to the US image histogram. For this test we manually initialize the model.

Figure 7: US LV segmentation (initialisation and final contour).

4 CONCLUSION

We have presented a segmentation framework to segment the LV (endorcadium/epicardium) in MRI (3D+T). Our fully automatic deformable model couples an edge-based energy (Kovesy asymmetry measure), a region-based energy (Local/Global Weibull model) and a shape-based energy (myocardium wall thickness). Our results, compared to a state of the art method, demonstrate the potential and reliability of our approach regarding our choices: not to include papillary muscle in the endocardium cavity and not to use strong priors in the model. Finally, we have illustrated the versatility of our method, by successfully segmenting ultrasound LV images, for multi-modal cardiac segmentation perspective.

REFERENCES

Aubert, G., Barlaud, M., Faugeras, O., and Jehan-Besson, S. (2003). Image segmentation using active contours: Calculus of variations or shape gradients? *SIAM Journal on Applied Mathematics*, 63(6):2128–2154.

Ayed, I. B., Hennane, N., and Mitiche, A. (2006). Unsupervised variational image segmentation/classification

using a weibull observation model. *Image Processing, IEEE Transactions on*, 15(11):3431–3439.

Barbosa, D. et al. (2013). Fast and fully automatic 3-d echocardiographic segmentation using b-spline explicit active surfaces: Feasibility study and validation in a clinical setting. *Ultrasound in Medicine & Biology*.

Belaid, A., Boukerroui, D., Maingourd, Y., and Lerallut, J.-F. (2011). Implicit active contours for ultrasound images segmentation driven by phase information and local maximum likelihood. In *Biomedical Imaging: From Nano to Macro, 2011 IEEE International Symposium on*, pages 630–635.

Caselles, V., Kimmel, R., and Sapiro, G. (1997). Geodesic active contours. *International journal of computer vision*, 22(1):61–79.

Chan, T. F. and Vese, L. A. (2001). Active contours without edges. *Image processing, IEEE transactions on*, 10(2):266–277.

Felsberg, M. and Sommer, G. (2001). The monogenic signal. *Signal Processing, IEEE Transactions on*, 49(12):3136–3144.

Foulonneau, A., Charbonnier, P., and Heitz, F. (2003). Geometric shape priors for region-based active contours. In *Image Processing, 2003. ICIP 2003. Proceedings. 2003 International Conference on*, volume 3, pages III–413.

Jolly, M.-P., Xue, H., Grady, L., and Guehring, J. (2009). Combining registration and minimum surfaces for the segmentation of the left ventricle in cardiac cine mr images. In *Medical Image Computing and Computer-Assisted Intervention–MICCAI 2009*, pages 910–918.

Kovesi, P. (1997). Symmetry and asymmetry from local phase. pages 2–4.

Lankton, S. and Tannenbaum, A. (2008). Localizing region-based active contours. *Image Processing, IEEE Transactions on*, 17(11):2029–2039.

Lu, Y., Radau, P., Connelly, K., Dick, A., and Wright, G. A. (2009). Segmentation of left ventricle in cardiac cine mri: An automatic image-driven method. In *Functional Imaging and Modeling of the Heart*, pages 339–347.

Paragios, N. (2002). A variational approach for the segmentation of the left ventricle in cardiac image analysis. *International Journal of Computer Vision*, 50(3):345–362.

Paragios, N. and Deriche, R. (2002). Geodesic active regions and level set methods for supervised texture segmentation. *International Journal of Computer Vision*, 46(3):223–247.

Pednekar, A., Kurkure, U., Muthupillai, R., Flamm, S., and Kakadiaris, I. A. (2006). Automated left ventricular segmentation in cardiac mri. *Biomedical Engineering, IEEE Transactions on*, 53(7):1425–1428.

Petitjean, C. and Dacher, J.-N. (2011). A review of segmentation methods in short axis cardiac mr images. *Medical image analysis*, 15(2):169–184.

Rajpoot, K., Noble, A., Grau, V., and Rajpoot, N. (2008). Feature detection from echocardiography images using local phase information. *Medical Image Understanding and Analysis*.

Sethian, J. A. (1999). *Level set methods and fast marching methods: evolving interfaces in computational geometry, fluid mechanics, computer vision, and materials science*, volume 3. Cambridge university press.